PHYSICAL REVIEW B **91**, 060511(R) (2015)

What superconducts in sulfur hydrides under pressure and why

N. Bernstein, C. Stephen Hellberg, M. D. Johannes, I. I. Mazin, and M. J. Mehl
Center for Computational Materials Science, Naval Research Laboratory, Washington, DC 20375-5000, USA
(Received 31 December 2014; published 27 February 2015)

The recent discovery of superconductivity at 190 K in highly compressed H_2S is spectacular not only because it sets a record high critical temperature, but because it does so in a material that appears to be, and we argue here that it is, a conventional strong-coupling BCS superconductor. Intriguingly, superconductivity in the observed pressure and temperature range was predicted theoretically in a similar compound, H_3S. Several important questions about this remarkable result, however, are left unanswered: (1) Does the stoichiometry of the superconducting compound differ from the nominal composition, and could it be the predicted H_3S compound? (2) Is the physical origin of the anomalously high critical temperature related only to the high H phonon frequencies, or does strong electron-ion coupling play a role? We show that at experimentally relevant pressures H_2S is unstable, decomposing into H_3S and S, and that H_3S has a record high T_c due to its covalent bonds driven metallic, which make this compound rather similar to MgB_2, but unlike most other good conventional superconductors.

DOI: 10.1103/PhysRevB.91.060511 PACS number(s): 74.20.Fg, 64.75.Nx, 74.20.Pq, 74.62.Fj

Recently reported superconductivity at 190 K in compressed H_2S [1] has been arguably the biggest discovery in the field since the superconducting cuprates nearly 30 years earlier. Superconductivity in a related compound, H_3S, in a similar range of pressure with very nearly the same critical temperature, was predicted theoretically [2] about a year earlier. In that theoretical paper, direct *ab initio* calculations yielded high phonon frequencies, giving the logarithmic average (the prefactor in the equation for T_c) on the order of 1100–1300 K and a coupling constant λ larger than 2, combining to give T_c between 191 and 204 K. However, a microscopic understanding of why this particular material features such a strong coupling is still missing, as is an explanation of the discrepancy between experimental and theoretical stoichiometries. As we show here, the answer lies in the stability of the H_nS series of compounds. At high pressure, the phase diagram favors decomposition of H_2S into H_3S and pure S. The mechanism of superconductivity can be traced to the strongly covalent metallic nature of H_3S along with high phonon frequencies, similar to another conventional (i.e., phonon-driven) superconductor with what now seems only a *relatively* high T_c, MgB_2 [3].

The discovery in 2001 of phonon-driven superconductivity at 39 K in MgB_2 not only set a record high T_c for a conventional phonon-mediated mechanism, which just 30 years back was widely believed to be limited to $\lesssim$25 K, but also introduced a completely new concept in the theory of superconducting materials, dubbed "doped covalent bonds" by Pickett and collaborators [4]. The essence of this concept is that bonding and antibonding states in a covalent system are very sensitive to hopping integrals and thus to ionic positions, which makes them strongly coupled to the corresponding phonons. However, in essentially all covalent systems, the corresponding states are removed from the Fermi surface and are thus irrelevant to superconductivity. Moreover, even when it is possible to dope a covalent insulator, such as diamond, it costs a tremendous amount of energy and therefore results in only very small doping levels. MgB_2 is different in two ways: First, it sports metallic π bands in addition to the strongly covalent σ bands; second, the σ bands are two dimensional (2D), and therefore even a small carrier concentration in these bands creates a sizable density of states (DOS), that is, a substantial covalent metallicity. In contrast, all the bands are three dimensional (3D) in diamond, and small doping causes a similarly small DOS, and thus a low critical temperature T_c.

While the general concept that hard phonons in H-rich materials might make them good superconductors is not new [5], so far high-T_c superconductivity has been elusive, primarily because such hard phonons normally do not produce large coupling constants. As Ginzburg wrote in 1977, "... in many already-known materials, the Debye temperature is very large, $\sim 10^3$ K, and low T_c is related to small coupling constants... In view of this, attention is attracted to various hydrogen-rich materials under high pressure" [6]. The strong electron-phonon coupling inherent to a covalent metal such as MgB_2 suggests a way to circumvent this problem, by combining metallized covalent bonds with lighter elements and higher phonon frequencies. We argue that H_3S applies precisely this recipe to achieve its record critical temperature and that the physics of superconductivity, and, to some extent, even numerics, in H_3S are extremely similar to MgB_2, with the only qualitative difference being the factor of 11 between the masses of H and B. Simply, H_3S is like MgB_2, but lighter. It is worth mentioning that before H_3S, other hydrates, for instance, H_3Ge, were predicted to show high T_c at even lower pressures [7], but these predictions were not realized, suggesting that H_3S is special in an important way. We argue here that the important feature of H_3S is the proximity in energy of the S *s*, S *p*, and H *s* orbitals at this pressure, which makes the bonding strongly covalent just as in MgB_2, while in H_3Ge, e.g., this is not the case and thus the analogy between MgB_2 and H_xGe, suggested in Ref. [8], is misleading.

To gauge the level of electron-phonon coupling, we note that the same electron-phonon interactions that contribute to phonon-mediated superconductivity also manifest themselves as the screening of bond-stretching force constants and softening of vibrations; this softening can therefore be taken as a proxy for the strength of the coupling. Recalling the case of MgB_2, we observe that it has covalent-bond-stretching phonons at about 500 cm^{-1} near the zone center, while in its sister compound AlB_2, which has its σ band far from the Fermi level and uncoupled from conducting electrons, those phonons are as hard as 900 cm^{-1} [9]. A softening of similar magnitude occurs in solid H_3S as compared with vibrations in S-H containing thiol molecules. The latter have frequencies of about 2500 cm^{-1}, while the calculated phonon frequencies in H_3S are roughly $\sim$1600 cm^{-1} [2]. This is a very large softening, indicating a very large coupling, even though it may not have been initially perceived as such because the bare frequency involving the light H atoms is so high.

In any theoretical analysis of a new material, it is important to establish the stoichiometry and the crystal structure of the compound of interest. For instance, some recent papers [10] are based upon the H_2S composition, which, as we show below, is almost certainly not the composition that supports superconductivity in the experiment. While the experiments showing superconductivity at 190 K started by compressing H_2S, they also showed the formation of pure S, suggesting that the material that actually superconducts is likely to be H enriched [1]. The composition that Duan *et al.* [2] studied theoretically, H_3S, is consistent with this observation, but they did not consider the full range of compositions in the phase diagram. Previous theoretical publications have verified that the proposed high pressure phases for H_3S in Ref. [2] and H_2S in Ref. [11] are stable against decomposition into H and S. However, the lack of decomposition into elemental species is not a particularly stringent test, and stability against separation into other phases, e.g., H_2S into S and H_3S, which is important for understanding the relevance of any calculations to the experiments in Ref. [1], was not studied in those publications.

We begin by checking the stability of H_nS compounds with respect to decomposition into other phases by calculating their zero temperature enthalpy $H = E + PV$ as a function of composition using density functional theory calculations. We used the VASP density functional theory software [12] with the Perdew-Burke-Enzerhoff generalized gradient approximation [13], and a projector-augmented wave (PAW) basis [14,15] with a 1000 eV plane wave cutoff. The calculations used $16 \times 16 \times 16$ Monkhorst-Pack k points for cells containing a single formula unit; correspondingly reduced k-point grids were used for the larger cells. Geometries were relaxed under an applied pressure using the conjugate-gradient algorithm applied to both unit cell size and shape, as well as atomic positions, until the residual forces were less than 0.01 eV/Å. Since the stability of each composition depends on the enthalpy of the *lowest enthalpy* structure at that composition, we considered many structures at compositions ranging from pure S, to H_nS for $n = 1$–6, to pure H. The initial structures for our relaxation procedure came from previously published experimental and computational studies [2,11,16–18], manual modifications of these published structures, and from a simple version of the random structure search method [19]. The final relaxed structures are listed in the Supplemental Material [20].

The zero temperature formation enthalpy of H_xS_{1-x}, $\Delta H(x) = H(x) - xH_H - (1-x)H_S$ as a function of x, is plotted in Fig. 1; we see that at $P = 200$ GPa, H_3S in the previously proposed body-centered-cubic (bcc) $Im\bar{3}m$ structure is stable with respect to decomposition into any of the other calculated structures. At 200 GPa the $R3m$ structure has cell and internal parameters that make it identical to the $Im\bar{3}m$, but below about 150 GPa it begins to continuously evolve to a distinct, lower symmetry structure [20]. All simulated H_2S

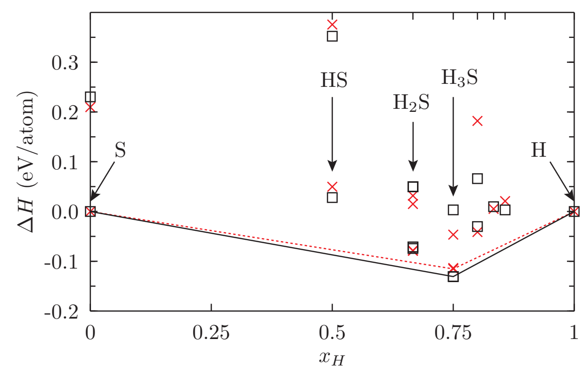

FIG. 1. (Color online) Formation enthalpy of H_xS_{1-x} as a function of H concentration at $P = 150$ GPa (red $\times$'s) and 200 GPa (black squares). Upper axis tick marks indicate compositions equivalent to H_nS for integer n. All compounds above the convex hull (lines) are unstable with respect to decomposition into the two adjacent phases on the convex hull. At both pressures the only stable compound is H_3S. Pure S structures are taken from Refs. [16,17], and pure H from Ref. [18]. The crystallographic description of these structures is given in the supplemental material [20].

structures, on the other hand, are unstable with respect to decomposition into S and H_3S by at least 120 meV/formula unit. All structures with higher H concentration lie above the convex hull, and are therefore also unstable with respect to decomposition into H_3S and H. In fact, all such structures include H atom pairs with distances similar to that of the H_2 molecule [20], showing the tendency to phase separation and release of pure H at these compositions. Note that small errors in the enthalpies of the end points (pure S and pure H), if, for example, the true structures are a bit lower in enthalpy than the ones we considered, will not change these conclusions with respect to the stability of H_3S and instability of all other compositions. However, it is in principle possible that a sufficiently lower enthalpy H structure could make all intermediate compositions unstable, or that a H_2S structure with enthalpy outside of the convex hull, which has not been considered here, could exist. We think that the existence of such a lower enthalpy structure is very unlikely for pure H, which has been studied extensively [18]. For H_2S, which is chemically reasonable and has not been studied extensively under such high pressure, we think that the failure of our thorough intuition-guided and random searches to find such a lower enthalpy structure makes its existence highly unlikely. Finally, higher H concentration phases show a tendency for the formation of H_2 molecules consistent with their predicted instability with respect to decomposition into pure H and H_3S. Reducing the pressure to 150 GPa does not significantly change the enthalpies of the low-lying structures. We therefore conclude that under experimentally relevant pressures the starting material H_2S decomposes as

$$3H_2S \rightarrow 2H_3S + S, \tag{1}$$

with no other products.

An important issue we have not addressed so far is the reliability of PAW calculations at such compressions since, generally speaking, the available PAWs were designed and tested for much larger interatomic separations. To this end, we compared

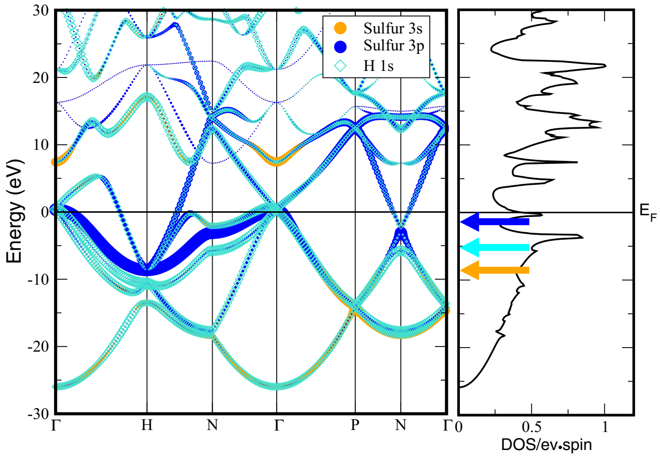

FIG. 2. (Color online) Band structure of the H_3S $Im\bar{3}m$ structure at $P = 200$ GPa, calculated using FPLO. Weights of the three most important atomic orbitals are shown with the symbols of the corresponding sizes, and arrows indicate FPLO on-site energies of each orbital. The large contribution of H orbitals to the S-s derived states at the bottom of the band indicates strong covalency.

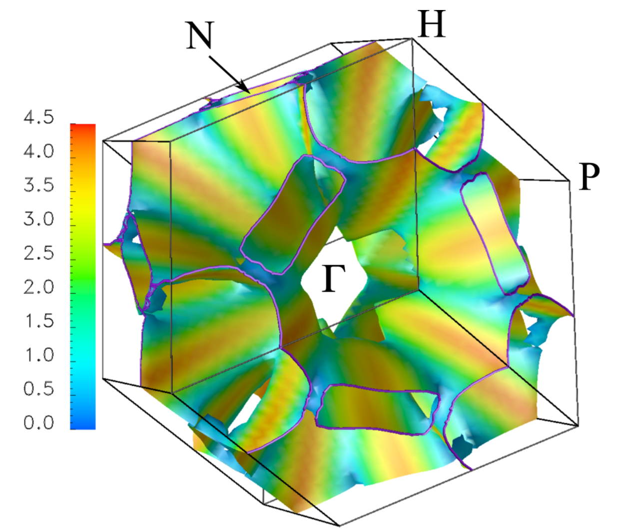

FIG. 3. (Color online) The main pocket of the Fermi surface of H_3S at $P = 200$ GPa, colored according to the local Fermi velocity (the scale is in arbitrary units). Note the heavy bands near the van Hove singularities. Two small hole pockets near Γ and an electron pocket near H contribute little to the total DOS, and are omitted from the picture.

the energy difference of the thermodynamic reaction (1) with the energy difference calculated with an all-electron method, full-potential local orbitals (FPLO) [21]. We found a formation energy of 105 meV/formula unit, within 10% of the VASP value, confirming that the latter calculations are reliable.

Having established that the material exhibiting superconductivity at 190 K at $P \sim 200$ GPa is most likely the $Im\bar{3}m$ bcc-like structure of H_3S identified in Ref. [2], we analyze its electronic structure and superconductivity. We do not aim at recalculating the exact numbers for the coupling constants and phonon frequencies, but rather at gaining insight into why the calculations of Ref. [2] produced such a large coupling and T_c.

In Fig. 2 we show our calculated band structure, which agrees with Duan *et al.* The Fermi surface for the one band (out of the five that cross the Fermi level) that contributes the overwhelming majority of the density of states, colored by the Fermi velocity, is shown in Fig. 3. The calculated average Fermi velocity, defined as $v_F = \sqrt{\Sigma_{\mathbf{k}}\delta(E_{\mathbf{k}} - E_F)v_{\mathbf{k}}^2/\Sigma_{\mathbf{k}}\delta(E_{\mathbf{k}} - E_F)}$, is 0.25×10^8 cm/s. This allows us to address another question: Given the large T_c, would the coherence length be long enough for the standard Eliashberg theory to be applicable? We know that in high-T_c cuprates this is nearly the case, which was argued to have important theoretical implications in terms of Bose condensation of local pairs rather than BCS long-range coherence [22]. For H_3S, we can estimate the zero temperature gap parameter $\Delta(0)$ using Carbotte's formula [23], $\Delta(0) = 1.76k_BT_c[1 + 12.5(T_c/\omega_{\log})^2\log(\omega_{\log}/2T_c)]$. Using the numbers from Ref. [2], we get $\Delta(0) \approx 40$ meV. Using the standard expression for the clean limit coherence length, $\xi = \hbar v_F/\pi\Delta(0)$, we find $\xi \sim 40$ Å, much larger than the interatomic distance.

Analyzing the characters of the wave functions as in Fig. 2, we observe that the bands at the Fermi level are formed nearly exclusively by seven orbitals: sulfur $3s$, sulfur $3p_{x,y,z}$, and the three $1s$ orbitals of the hydrogens, each displaced along x, y, or z from its nearest-neighbor sulfur. The S d states are located more than 15 eV above the Fermi level and can be safely neglected. In the following we will denote the three hydrogen $1s$ orbitals by $i = x,y,z$, and the three sulfur p orbitals by $I = X,Y,Z$, and the sulfur s by just s. The nearest-neighbor S-H Hamiltonian is

$$H_{si} = t_a C_i, \tag{2}$$

$$H_{Ii} = t_b S_i, \tag{3}$$

where $t_{a,b}$ are the $ss\sigma$ and $ps\sigma$ S-H hoppings, respectively, $C_i = 2\cos(k_i a/2)$, and $S_i = 2\sin(k_i a/2)$. The H-H nearest-neighbor hopping, despite this distance being the same as the S-H one, is much smaller, due to the difference in radii of the H $1s$ and S $3s$ orbitals. The H-H Hamiltonian can be written down as

$$H_{xy} = t_c \exp[i(k_x - k_y)a/2]C_z, \tag{4}$$

etc. Using FPLO to construct these Wannier functions and their corresponding tight-binding Hamiltonian, we find $t_a = -4.2$ eV, $t_b = -5.2$ eV, and $t_c = -2.7$ eV. The on-site energies are $E_{3s} = -8.6$ eV, $E_{3p} = -1.3$ eV, and $E_{1s(\mathrm{H})} = -5.0$ eV (E_F set to zero). As indicated by the arrows in Fig. 2, these three orbitals are close in energy as compared with the valence band width, and the hydrogen s level lies between the two sulfur levels, creating strong covalent bonds with both. The calculated bonding-antibonding splitting between sulfur p and hydrogen s states at the P point ($k = \{\pi/4a,\pi/4a,\pi/4a\}$) is $2\Delta \approx 25$ eV. However, the same splitting, by symmetry, is zero at the Γ point, so, despite very strong covalency, this bond remains metallic, with the DOS $N(0) \sim 0.6$ states/eV.

It is now instructive to compare these parameters with those in MgB_2, keeping only bond-stretching boron phonons in MgB_2 and bond-stretching H phonons in H_3S; in both cases these contributed about 70% to the total coupling (it is worth noting that a 30% contribution to the coupling constants does not imply a comparable contribution to T_c; in fact, since $\omega_{\log} = \omega_S^{0.3}\omega_H^{0.7}$, excluding sulfur phonons would lead to very small changes in T_c). In order to do so, we use the well-known qualitative relations between the electron-phonon coupling constant λ, its electronic part (also called the Hopfield factor) η, and the average force constant Φ. For the purpose of the ensuing discussion it is enough to know that the Hopfield factor η characterizes the electron-ion interaction and depends only on electronic properties, such as the DOS and the ionic potential, but not on phonon frequencies, while Φ is defined in such a way [24] that it represents a combination of the derivatives of total energy with respect to ionic coordinates (force constants) and thus carries information about the phonon spectrum, but does not directly depend on the electronic energies and wave functions. On a semiquantitative level [25],

$$\lambda \approx \eta/\Phi, \tag{5}$$

$$\Phi = \Phi_0 - 2\eta. \tag{6}$$

Here Φ_0 represents unscreened force constants that do not account for electron-phonon coupling. Note that if there is one dominant phonon mode, $\Phi_0/\Phi \approx \omega_0^2/\omega^2$, where ω and ω_0 are the screened and unscreened frequencies of this mode, respectively. Using the bond-stretching mode frequencies for AlB_2 and MgB_2 to represent unscreened and screened bonds, respectively, as mentioned above, we get

$$\Phi_0/\Phi \approx (900/500)^2 \sim 3, \tag{7}$$

$$\lambda \approx \frac{1}{2}\left(\frac{\Phi_0}{\Phi} - 1\right) \approx 1, \tag{8}$$

which qualitatively agrees with the accepted values for MgB_2 [3], $\lambda_{\sigma\sigma} = 0.78$–$1.02$. This gives

$$\eta_{MgB_2} \approx 1 \times 11 m_H \times (500\ \mathrm{cm}^{-1})^2 \tag{9}$$

$$\sim 2.75 \times 10^6 m_H\ \mathrm{cm}^{-2}. \tag{10}$$

If we assume the same Hopfield factor η for H_3S, we get $\lambda \approx 2.75 \times 10^6/1300^2 \approx 1.6$ (estimating the average frequency of the bond-stretching modes in H_3S from Fig. 5 in Ref. [2] as 40 THz), which is not far from the value $\lambda = 2.19$ reported in Ref. [2]. Note that the logarithmic frequency in that paper was calculated to be 930 cm^{-1}, suggesting that phonons softer than 40 THz contribute to total coupling. Had we taken $\omega = 1100$ cm^{-1} = 35 THz instead of 40 THz, we would have obtained the value calculated in Ref. [2].

As a consistency check, let us now see whether this estimate implies a plausible number for Φ_0. Using $\omega = 1300$ cm^{-1} and $\lambda = 1.6$, we find $\omega_0 \approx 1300\sqrt{1 + 2 \times 1.6} = 2660$ cm^{-1}, consistent with the vibron frequencies in S-H molecules, which have a large gap and are unscreened by definition. The internal consistency of our analysis and its consistency with experiment confirm our main conclusions below.

In conclusion, at a pressure of $P = 200$ GPa, H_2S gains nearly 40 meV per atom by decomposing into elemental sulfur and H_3S in the $Im\bar{3}m$ structure. The physical mechanism underlying the high-temperature superconductivity of H_3S at that pressure is very similar to that in MgB_2: metallization of covalent bonds. The main difference from MgB_2 is that the hydrogen mass is 11 times smaller than the mass of boron, resulting in a 3.5 times larger prefactor.

Note added. Recently, we became aware of several articles [26–28] that confirmed our DFT results using different structural search techniques.

We acknowledge useful discussions with D. A. Papaconstantopoulos and M. Calandra. This research was funded by the Office of Naval Research through the Naval Research Laboratory's basic research program. Computations were performed at the AFRL and ERDC DoD Supercomputing Resource Centers.

[1] A. P. Drozdov, M. I. Eremets, and I. A. Troyan, arXiv:1412.0460.
[2] D. Duan, Y. Liu, F. Tian, D. Li, X. Huang, Z. Zhao, H. Yu, B. Liu, W. Tian, and T. Cui, Sci. Rep. **4**, 6968 (2014).
[3] For a review, see I. I. Mazin and V. P. Antropov, Physica C **385**, 49 (2003).
[4] J. M. An and W. E. Pickett, Phys. Rev. Lett. **86**, 4366 (2001).
[5] See, e.g., N. W. Ashcroft, Phys. Rev. Lett. **21**, 1748 (1968).
[6] *Problema Vysokotemperaturnoi Sverkhprovodimosti—The Problem of High-Temperature Superconductivity*, edited by V. L. Ginzburg and D. A. Kirzhnits (Nauka, Moscow, 1977) [English translation: High-Temperature Superconductivity (Consultants Bureau, New York, 1982)].
[7] K. Abe and N. W. Ashcroft, Phys. Rev. B **88**, 174110 (2013).
[8] N. W. Ashcroft, Phys. Rev. Lett. **92**, 187002 (2004).
[9] K.-P. Bohnen, R. Heid, and B. Renker, Phys. Rev. Lett. **86**, 5771 (2001).
[10] J. E. Hirsch and F. Marsiglio, arXiv:1412.6251; A. P. Durajski, R. Szczesniak, and Y. Li, arXiv:1412.8640.
[11] Y. Li, J. Hao, H. Liu, Y. Li, and Y. Ma, J. Chem. Phys. **140**, 174712 (2014).
[12] G. Kresse and J. Furthmüller, Comput. Mater. Sci. **6**, 15 (1996); Phys. Rev. B **54**, 11169 (1996).
[13] J. P. Perdew, K. Burke, and M. Ernzerhof, Phys. Rev. Lett. **77**, 3865 (1996); **78**, 1396 (1997).
[14] P. E. Blöchl, Phys. Rev. B **50**, 17953 (1994).
[15] G. Kresse and D. Joubert, Phys. Rev. B **59**, 1758 (1999).
[16] H. Luo, R. G. Greene, and A. L. Ruoff, Phys. Rev. Lett. **71**, 2943 (1993).
[17] O. Degtyareva, E. Gregoryanz, M. Somayazulu, P. Dera, H.-K. Mao, and R. J. Hemley, Nat. Mater. **4**, 152 (2005).
[18] C. J. Pickard and R. J. Needs, Nat. Phys. **3**, 473 (2007).
[19] C. J. Pickard and R. J. Needs, J. Phys.: Condens. Matter **23**, 053201 (2011).
[20] See Supplemental Material at http://link.aps.org/supplemental/10.1103/PhysRevB.91.060511 for the lattice and atomic parameters, as well as enthalpies, of all relaxed low energy structures.

[21] K. Koepernik and H. Eschrig, Phys. Rev. B **59**, 1743 (1999); I. Opahle, K. Koepernik, and H. Eschrig, *ibid.* **60**, 14035 (1999).

[22] See, e.g., Q. J. Chen, J. Stajic, S. Tan, and K. Levin, Phys. Rep. **412**, 1 (2005).

[23] J. P. Carbotte, Rev. Mod. Phys. **62**, 1027 (1990).

[24] *Problema Vysokotemperaturnoi Sverkhprovodimosti—The Problem of High-Temperature Superconductivity* (Ref. [6]), Eq. (4.77).

[25] *Problema Vysokotemperaturnoi Sverkhprovodimosti—The Problem of High-Temperature Superconductivity* (Ref. [6]), Eq. (3.75).

[26] D. Duan, X. Huang, F. Tian, D. Li, H. Yu, Y. Liu, Y. Ma, B. Liu, and T. Cui, arXiv:1501.01784.

[27] I. Errea, M. Calandra, C. J. Pickard, J. Nelson, R. J. Needs, Y. Li, H. Liu, Y. Zhang, Y. Ma, and F. Mauri, arXiv:1502.02832.

[28] J. A. Flores-Livas, A. Sanna, and E. K. U. Gross, arXiv:1501.06336.